

See discussions, stats, and author profiles for this publication at: <https://www.researchgate.net/publication/230208843>

Photocatalytic reactors for environmental remediation: A review

ARTICLE *in* JOURNAL OF CHEMICAL TECHNOLOGY & BIOTECHNOLOGY · AUGUST 2011

Impact Factor: 2.35 · DOI: 10.1002/jctb.2650

CITATIONS

48

READS

72

4 AUTHORS, INCLUDING:



Cathy McCullagh

The Robert Gordon University

26 PUBLICATIONS 349 CITATIONS

SEE PROFILE



Nathan Skillen

Queen's University Belfast

4 PUBLICATIONS 53 CITATIONS

SEE PROFILE



Morgan Adams

The Robert Gordon University

16 PUBLICATIONS 106 CITATIONS

SEE PROFILE

Photocatalytic reactors for environmental remediation: a review

Cathy McCullagh, Nathan Skillen, Morgan Adams and Peter K.J. Robertson*

Abstract

Research in the field of photocatalytic reactors in the past three decades has been an area of extensive and diverse activity with an extensive range of suspended and fixed film photocatalyst configurations being reported. The key considerations for photocatalytic reactors, however, remain the same; effective mass transfer of pollutants to the photocatalyst surface and effective deployments and illumination of the photocatalyst. Photocatalytic reactors have the potential versatility to be applied to the remediation of a range of water and gaseous effluents. Furthermore they have also been applied to the treatment of potable waters. The scale-up of photocatalytic reactors for waste and potable water treatment plants has also been demonstrated. Systems for the reduction of carbon dioxide to fuel products have also been reported. This paper considers the main photocatalytic reactor configurations that have been reported to date.

© 2011 Society of Chemical Industry

Keywords: photocatalyst; reactor; fluidized bed; immobilized film; suspended catalyst mass transport; rate control

INTRODUCTION

The application of semiconductor photocatalysis in the fields of engineering and science is an important area of research, which has grown significantly in the last three decades with increasing numbers of publications appearing every year.^{1–6} Semiconductor photocatalysis has been applied to a diverse array of environmental problems including air, potable, and wastewater treatment. This versatile process has also been utilized for the destruction of micro-organisms such as bacteria,^{6,7} viruses⁸ and for the inactivation of cancer cells.^{9,10} Semiconductor photocatalysis has also been applied to the photo-splitting of water to produce hydrogen gas,^{11–14} nitrogen fixation^{15–18} and for the remediation of oil spills.^{19–21}

Heterogeneous photocatalysis for the remediation of polluted water streams falls into two distinct areas. First, the focus is on basic chemical transformations on semiconductor photocatalyst materials. These investigations have concentrated on the examination of basic photocatalytic processes including photocatalytic material science, surface interactions on photocatalysts, reaction mechanisms, and kinetics that impact on the processes on a molecular level.^{1–5}

In order to demonstrate the viability of semiconductor photocatalysis for environmental remediation, reactor design is an equally critical factor. Effective reactor design research and development aims to scale up laboratory bench scale processes to industrially feasible applications. Scaling up photocatalytic reactors is, however, a complex process with many factors needing consideration to yield a technically and economically efficient process. These factors include distribution of pollutant and photocatalyst, pollutant mass transfer, reaction kinetics, and irradiation characteristics. The issue of effective photocatalyst illumination is particularly important as this essentially determines the amount of water that may be treated per effective unit area of deployed photocatalyst. A wide range of photocatalytic reactors have been developed and used in both basic research and pilot

scale studies. The central problem of scale-up of photocatalytic reactors is the provision of sufficient high specific surface area of catalyst and the uniform distribution of illumination across this area.

MECHANISM OF HETEROGENEOUS PHOTOCATALYSIS

As a process for water purification, photocatalysis has numerous advantages over many existing technologies. The technique can result in the mineralization of pollutants rather than transferring them to an alternative phase, such as is the case with activated carbon adsorption. Furthermore, photocatalysis does not require the use of hazardous materials such as hypochlorite, peroxide or ozone.⁴ Titanium dioxide (TiO₂) is the catalyst of choice as it is inexpensive, non-toxic, chemically stable and is highly photocatalytically active.² TiO₂ acts as a photocatalyst due to its electronic structure, characterized by an electronically filled valence band and empty conduction band²² separated by a band gap. If a photon of energy greater than or equal to the bandgap energy, E_g , is absorbed by TiO₂, an electron is promoted from the valence band to the conduction band. This generates a reducing electron in the conduction band and an oxidizing hole in the valence band (Fig. 1). The excited conduction band electrons may recombine with the valence band holes generating heat energy. Alternatively they may be trapped in surface states and undergo reactions with electron donating or accepting species

* Correspondence to: Peter K.J. Robertson, IDEaS, Innovation, Design and Sustainability Research Institute, Robert Gordon University, Schoolhill, Aberdeen, AB10 1FR, UK. E-mail: peter.robertson@rgu.ac.uk

IDEaS, Innovation, Design and Sustainability Research Institute, Robert Gordon University, Aberdeen, UK

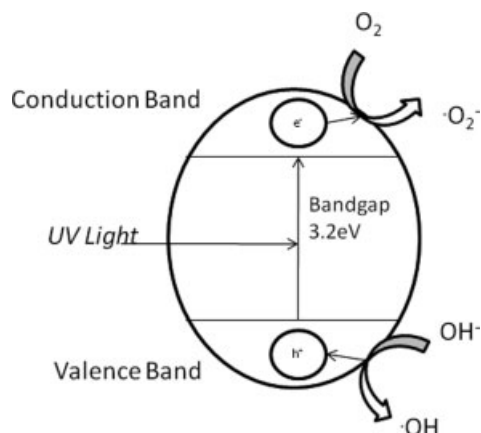


Figure 1. Processes that occur on photo-excitation of TiO_2 .

that are adsorbed on the TiO_2 surface. The electron and holes formed are highly charged and can induce redox reactions, which can ultimately result in the mineralization of aqueous pollutants. Hydroxyl radicals are believed to be generated on the surface of TiO_2 through a reaction of the valence band holes with adsorbed water, hydroxide or surface titanol groups (Equation (2)). The photogenerated conduction band electrons react with electron acceptors such as oxygen which generates superoxide ($\text{O}_2^{\bullet-}$) (Equation (4)). Thermodynamically the redox potential of the TiO_2 electron/hole pair should enable the production of hydrogen peroxide, primarily via the reduction of adsorbed oxygen^{3,23,24} (Equations (1)–(7)).

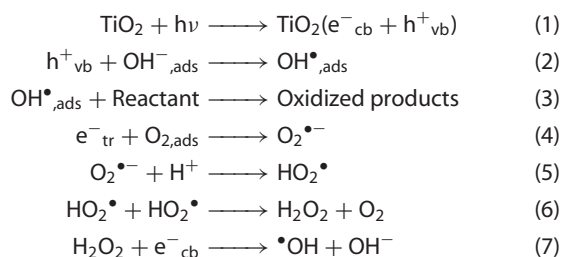


Figure 1 illustrates the basic processes involved in photocatalysis.

TYPES OF REACTOR CONFIGURATIONS

A wide variety of reactor configurations have been reported in the literature over the past 30 years including:

- annular photoreactor,^{25,26}
- packed bed photoreactor,²⁷
- photocatalytic Taylor vortex reactor,^{28–31}
- fluidised bed reactor,^{32,33}
- coated fibre optic cable reactor,³⁴
- falling film reactor,³⁵
- thin film fixed bed sloping plate reactor,³⁶
- swirl flow reactor,³⁷
- corrugated plate reactor.³⁸

Table 1 shows a comprehensive yet not exhaustive overview of photoreactor type, reactant phase, experimental targets, catalyst employed, and industrial applications.

Examples of these various reactors will be considered in the following sections.

Suspended liquid reactors

Slurry/suspension systems

TiO_2 catalysts have been investigated in both slurry/suspension systems and immobilized systems. The main advantage of using photocatalyst slurries is the larger surface area compared with the immobilized system. The separation of the nanometre catalyst particles is, however, expensive and is a major drawback in the commercialization of this type of system.³⁹ Nan Chong *et al.*⁴⁰ have reported the use of H-titanate nanofibres in an annular slurry photoreactor. They studied congo red as a model compound and showed that one of the key advantages was the settling velocity of the catalyst. Using Kynch's theory batch settling trials revealed that the H-titanate nanofibre photocatalysts resulted in a settling velocity of $8.38 \times 10^{-4} \text{ m s}^{-1}$. The authors proposed that these novel nanoparticles could deliver a true engineering solution to catalyst separation on an industrial scale. It was also reported that it was difficult to effect irradiation of all the photocatalyst particles in the slurry in the unit due to shielding from the light source of particles in the body of the unit by particles closer to the reactor walls. Therefore depth of light penetration into the slurry reactor was restricted.

It has been reported that the ratio between backward reflected and incident photon flow is strongly influenced by the geometry within the reactor. The Apparent Napierian Extinctance (ANE) coefficient for slurries is a parameter that is related to the photon absorption rate.⁴¹ ANE depends on the particle size and is inversely proportional to the particle size where:

$$(\text{ANE})_{\lambda} = -\ln(I/I_0) \quad (8)$$

where I is the outgoing light intensity after interaction with catalyst suspension and I_0 represents the light intensity obtained in a blank setup. The absorption of light within slurry systems cannot be separated from scattering, which makes kinetic analysis of experiments more challenging.⁴²

An alternative approach is to attach the catalyst to a transparent stationary support over which the contaminated water passes. In such a system it is possible to achieve effective illumination of all the photocatalyst deployed in the reactor.^{43,44} There are, however, problems associated with immobilized systems, which include the dependence on mass transfer of pollutant to the photocatalyst surface and ensuring effective access to the photocatalyst surface of both activating photons and reacting molecules.⁴⁵ The photocatalyst film thickness may affect the internal mass transfer as it may not be possible to access the photocatalyst material in the proximity of the support–catalyst interface. Each of these factors will result in a reduction in the rates of decomposition in immobilized film photocatalyst units when compared with slurry processes.

An early slurry based reactor effected the complete mineralization of chloroform to chloride and CO_2 .⁴⁶ This study was further supported by Kormann *et al.*⁴⁷ who demonstrated the complete dehalogenation of chloroform but also illustrated an increase in $[\text{Cl}^-]$ as a function of time. Pramauro *et al.*⁴⁸ reported the complete degradation of monuron (Fig. 2(a)), a persistent herbicide, within 1 h of photocatalysis. The reaction conditions investigated were simulated solar irradiation, TiO_2 slurry, and a batch reactor. Several intermediate products were determined after 30 min irradiation; these were not detected at the end of the irradiation time. The complete degradation and dechlorination of 3,4-dichloropropionamide (Fig. 2(b)), another persistent herbicide,

Table 1. Overview of photoreactor type, reactant phase, experimental targets, catalyst employed, and industrial applications

Reactor Type	Reactant phase	Reactor name	Experimentation	Catalyst used	Industrial application/Comments	Reference
Immobilized	Liquid	Photocatalytic Membrane Reactor (PMR)	Azo dye degradation	Anatase-phase TiO ₂		104
		Fixed Bed	Waste water treatment	TiO ₂		105
		Corrugated plate	4-chlorophenol degradation	TiO ₂ (P25)		38
		Rotating Disc	4-chlorobenzoic acid degradation	TiO ₂ (coated commercial ceramic and glass balls)		81
		Carberry photoreactor	4-chlorophenol degradation	TiO ₂ (P25) on sodium glass support.		106
	Gas	Optical Fibre Reactor (OFR)	Degradation of 4-chlorophenol	TiO ₂ on quartz fiber cores	Water treatment	34
		Annular Wall	PCE degradation	TiO ₂	Air purification	101
		Circulated system	CO ₂ reduction	TiO ₂ (P25), ZrO ₂		107
		Monolith	Cyclohexane	TiO ₂ (Hombikat UV100)	Air purification	91
		Carbon foam-based photoreactor	Gaseous methanol oxidation	TiO ₂ (P25) supported on carbon foam		94
Suspended	Vapour	Photocatalysis-ultrafiltration reactor (PUR)	Fulvic acid	TiO ₂ (P25)		108
		Rotating drum reactor	Hydrocarbons	TiO ₂ (P25)	Waterwater treatment. Drinking water disinfection.	56
	Liquid	Taylor vortex	Formate acid	TiO ₂ (P25)		29
		Fountain	Indigo carmine oxidation	TiO ₂		109
		Falling film slurry	Salicylic acid oxidation	TiO ₂ (P25)		51
		Internally circulating slurry bubble column reactor	Hydrogen production	CdS		110
		Cocurrent downflow contactor reactor (CDCR)	TCE	TiO ₂ (P25)		53
		Hybrid low-pressure submerged membrane photoreactor	2,4,6-trichlorophenol (2,3,6-TCP)	TiO ₂ (VP Aeroperl P25/20)		111
		Hybrid photoreactor	Removal of bisphenol A	TiO ₂ (P25)		112
		Slurry reactor-immersed membrane	Azo dye – reactive blue 69	TiO ₂ (P25)	Wastewater treatment. Uses Solar irradiation	113
		Novel labyrinth bubble photocatalytic reactor	Synthetic wastewater	TiO ₂ (P25)	Wastewater Treatment	114
		Fluidized bed photoreactor	Methyl orange degradation	TiO ₂ immobilized on quartz glass. (Used in suspension)	Wastewater treatment. Built on a commercial scale.	115
		Standard slurry photoreactor	MC-LR destruction	TiO ₂ coated activated carbon		33
			Methylene blue degradation	AgBr/nanoAIMCM-41	Visible light activated.	116
			Methyl orange oxidation	p-CaFe ₂ O ₄ /n-Ag ₃ VO ₄	Visible light activated.	117
			Hydrogen production	Ag ₂ Mo ₄ O ₁₃		118
				Nb ₂ Zr ₆ O ₁₇ – xNx	Visible light activated	119
				Cu ₂ WS ₄	Visible light activated	120
				ZnIn ₂ S ₄	Visible light activated	121

was reported by Pathirana and Maithreepala⁴⁹ using a TiO₂ suspension photocatalytic reactor. It was reported that dechlorination of the herbicide was dependent on TiO₂ concentration, and higher photocatalyst levels caused a shielding effect of the incident light. Li Puma and Yue⁵⁰ investigated the kinetics of degradation of single component and multi-component systems of chlorophenols. They studied the simultaneous use of short, medium, and long wavelength ultra-violet light to investigate the integration of simultaneous photocatalysis and photolysis. The optimal loading of photocatalyst for the geometry of their batch reactor via the oxidation of 2-CP to CO₂ was determined as part of this investigation, with mineralization rates achieving a three-fold increase up to a maximum photocatalyst loading of 0.5 mg L⁻¹. In the single component experiments the kinetics were too complex to allow the authors to determine whether the photolytic pathway would be preferential to the photocatalytic pathway or vice versa. During the multi-component experiments they observed that the overall oxidation kinetics were controlled by the reactant in excess, as the substrate present in smaller concentrations was found to degrade at a much slower rate than that in the single-component experiments. Overall the authors demonstrated that the entire course of photocatalytic oxidation of single-component and multi-component systems of chlorophenols can be predicted satisfactorily using simple kinetic models that could be useful in the design and modelling of large-scale photocatalytic reactors. This work was followed by studies of a pilot-scale continuous-flow laminar falling film slurry photocatalytic reactor (LFFSIW),⁵¹ which utilized commercially available UV lamps. A comprehensive investigation of this unit was reported looking at a range of parameters, including the wavelength and intensity of the incident irradiation source, the influence of additional oxidizing reagents, the concentrations of both reactants and photocatalyst, and the irradiation time. Li Puma and Yue also studied six different photon based processes, and determined that the UVC photocatalysis/UVC photolysis/UVC peroxidation process was superior to UVA photocatalysis, UVC photocatalysis/UVC photolysis, UVA photocatalysis/UVA peroxidation, UVC photolysis/UVC peroxidation and UVC photolysis systems. The results of the experiments conducted at different incident radiation intensities clearly indicated that low-wattage UVC lamps were preferable to high-wattage UVC lamps because enhancements of reactor conversions due to higher lamp power were offset by an increase in electricity costs.

Further work by Li Puma and Yue³⁵ compared the effectiveness of a range of photooxidation processes in a falling film pilot reactor. They investigated UVA-photocatalysis, UVA-photocatalysis-peroxidation, UVC-photolysis, UVC-photolysis-peroxidation, UVC-photocatalysis-photolysis and UVC-photocatalysis-photolysis-peroxidation. They selected salicylic acid as a model compound for all experiments. The highest conversion of salicylic acid was 58%, which was obtained with the UVC-photolysis-peroxidation process. Conversely the highest conversion to CO₂ was obtained with the UVC-photocatalysis-photolysis-peroxidation process (28%) and the lowest value was with the UVA-photocatalysis process (1.7%). The mineralization efficiency of the photocatalytic and the photolytic-photocatalytic processes was in the range 58–65%, far above that of the photolytic process which was in the range of 14–18%.

San *et al.*⁵² investigated the photodegradation of 3-aminophenol (3-AP) in a TiO₂ batch suspension photoreactor. They reported that this process followed pseudo-first-order kinetics, with the apparent rate constant depending on the initial 3-AP

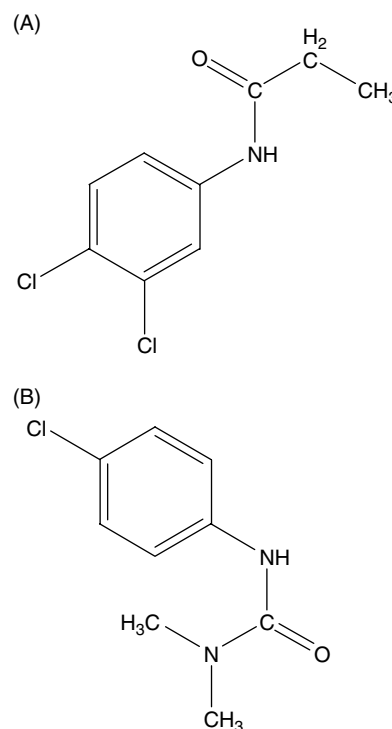


Figure 2. Chemical structure of the herbicides Monuron and 3,4-dichloropropionamide.

concentration. Furthermore, the addition of electron acceptors enhanced the reaction rate significantly.

A study of the adsorption and photocatalytic degradation of the safrina HEXL dye, has been reported using a TiO₂ slurry reactor.⁵³ The authors concluded that dye adsorption to the photocatalyst surface was critical for efficient photocatalytic degradation. The process was also pH dependent with an improved degradation rate observed near the point of zero TiO₂ charge. The TiO₂ slurry catalyst has also been employed within an internally circulating bubble column reactor for the degradation of trichloroethylene, with a removal efficiency of 97% reported.⁵⁴ Employing photocatalyst filtration with a bubble column reactor and TiO₂ slurry may be an efficient process for the destruction of phenoxyacetic acid.⁵⁵ This overcomes one of the major drawbacks of slurry systems, separation of catalyst from the remediated waste stream.

Adams *et al.*⁵⁶ reported the comparison of a standard flat plate reactor with a novel drum reactor⁵⁷ for the removal of oil and gas hydrocarbon contaminants from water. The flat plate design was constructed from polymethylmethacrylate (PMMA) and was a small-scale laboratory unit, however, a 'concertina' designed reactor was proposed for scale up. The drum reactor concept was a single pass continuous flow system for the treatment of wastewater/effluents, which utilized rotating paddles to ensure an even distribution of catalyst⁵⁶ (Fig. 3).

The reactor set up utilized three connecting drum reactors. The paddles positioned on the inside of the reactor drum were placed to allow the removal of pellets from the reaction solution for exposure to UV illumination before returning to the main stock.^{56,57} Depending on the level of contaminant present the effluent would pass from one 'drum' to another for prolonged treatment. On average the sample would reside in each drum for approximately 3 min with an overall reaction time of approximately 10 min. In the event of the final sample still

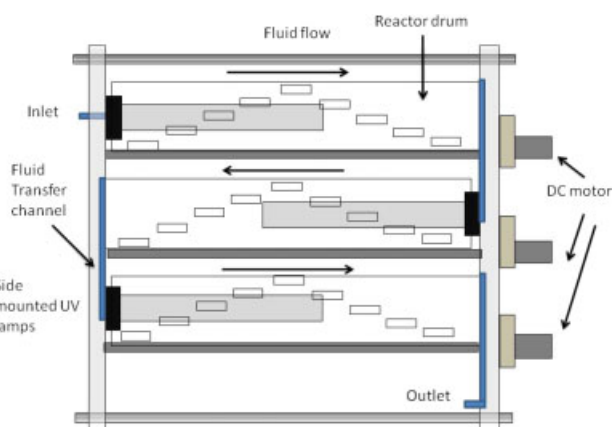


Figure 3. Schematic of photocatalytic drum reactor. (Reproduced from reference 58 with permission from Elsevier).

being of high hydrocarbon concentration the effluent would be recirculated into the system. As an attempt to develop a reactor deemed more environmentally efficient, pelletized catalyst was used to reduce downstream processing restrictions associated with the filtration of powdered catalyst. While both designs proved effective in the removal of hydrocarbons the drum reactor achieved 90% removal in less than 10 min. This high level of reduction over a short period of time is attributed to samples passing through three consecutive drums each with 200 g of TiO_2 catalyst present, therefore utilizing 600 g for the entire system. The flat plate design was investigated with regard to optimizing conditions to provide maximum destruction. It was concluded that a lower angled plate increases retention times of compounds and thus the chance of successful catalyst–pollutant interface.⁵⁶ The addition of air and hydrogen peroxide to increase destruction proved effective, with 80% degradation over 135 min recorded for H_2O_2 compared with 40% for air alone.

A subsequent paper McCullagh *et al.*⁵⁸ described the degradation of methylene blue (MB) in a slurry continuous flow drum reactor (Fig. 4(A)): 98% degradation of MB over 60 min of illumination utilizing a high loading weight of 30 g L^{-1} of TiO_2 pellets was reported. The investigation of different loading weights concluded that a maximum weight of 180 g of catalyst was attainable. While 98% degradation was recorded for 30 g catalyst (pellet form) over 60 min, the use of Degussa P25 as a photocatalyst was significantly more efficient, with 90% of the MB decomposed within 20 min photocatalysis (Fig. 4(B)).

Further evaluation of the drum reactor has been carried out in the remediation of oily waste water (OWW) from an interceptor tank.⁵⁹ In this study the unit achieved a 50% reduction in abundance for both decane and dodecane after 90 min photocatalysis along with >50% abundance reduction in tetradecane. Following a further 90 min illumination period of the OWW in the reactor all volatile organic compounds (VOC) initially identified were almost completely removed. Additionally total organic carbon TOC was investigated showing a 35% reduction in TOC for OWW samples passed twice through the reactor. The results highlighted demonstrate a high efficiency for a novel photocatalytic reactor with large scale applications as a polishing technique to be coupled with current water treatment processes.⁵⁹

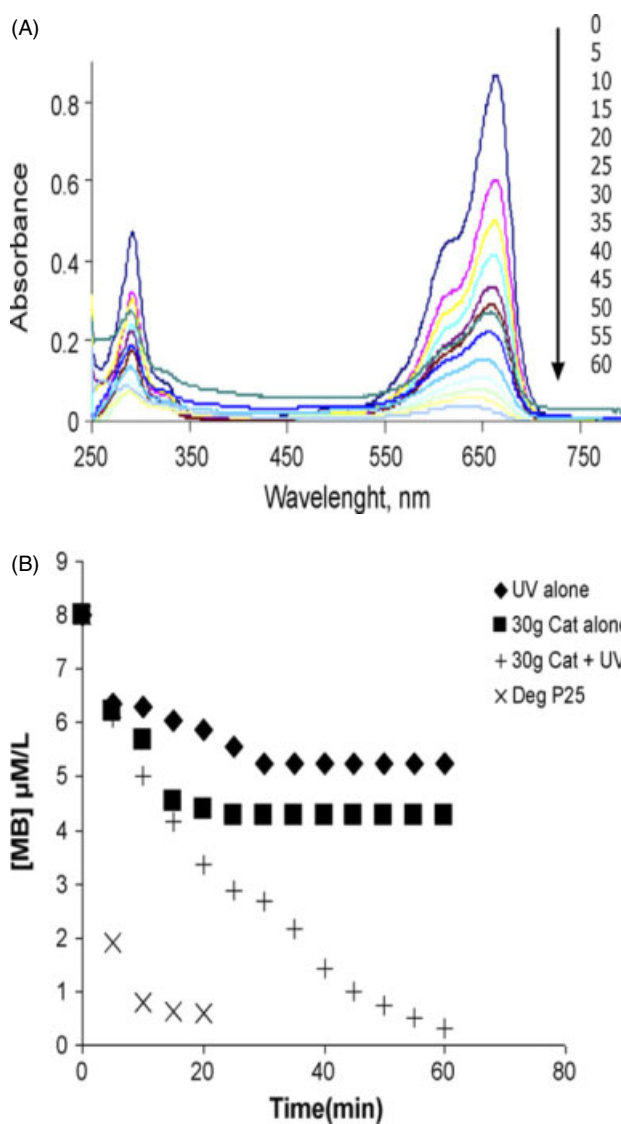


Figure 4. (A) Temporal absorption spectral pattern displaying the degradation of MB over a 60 min time period and (B) effect of UV only, 30 g catalyst (pellet form) only, UV combined with 30 g catalyst and Degussa P25 (powder) effect on MB degradation. (Reproduced from reference 58 with permission from Elsevier).

Mass transfer limitations within TiO_2 slurry reactors

Mass transfer within slurry reactors has not received a great deal of attention primarily because such problems have not been recognized as being major impediments to the application of a slurry reactor. Chen and Ray⁶⁰ did not observe either intra or extra particle diffusive limitations when working with a suspended solid reactor. Considering the optical thickness of the suspension Martin *et al.*⁶¹ found a loss in reactor efficiency when the optical thickness of the suspension was greater than a calculated optimum level. For large catalyst loading, restrictions on mass and radiation transport inside the catalytic particle have been reported by Mehrotra *et al.*⁶² Peralta Muniz Moreira⁶³ found no diffusion limitations within their reactor when pseudo-first-order kinetics were applied along with the Weiz and Prater criterion. How mass transport influences the rate of reaction within slurry reactors is very important in order to obtain relevant kinetic information about the reaction but also for photoreactor design. Ballari *et al.*⁶⁴ investigated the effects

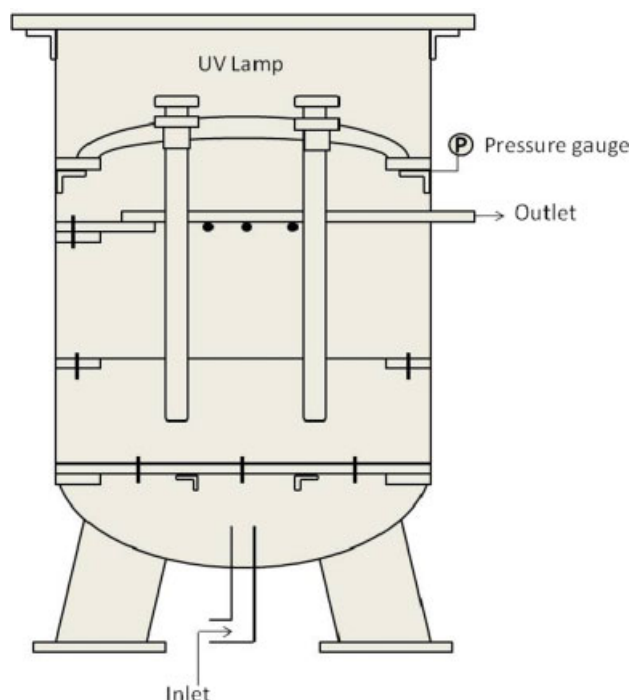


Figure 5. Schematic of fluidized bed reactor utilized for the destruction of microcystin-LR. (Reproduced from reference 33 with permission from Elsevier).

of photocatalyst irradiation, photocatalyst loadings, flow rates, total suspension volume, and changes in illumination length of the reactor. They found significant concentration gradients that were likely to cause limitations in mass transport resulting from the non-uniformity of the irradiation area. The authors state that these concentration gradients are difficult to avoid but could be eradicated if fully developed turbulent flow operated within the reactor. They concluded that mass transport problems could be overcome using a 1 g L^{-1} catalyst loading, irradiation rates of $1 \times 10^{-7} \text{ Einsteins cm}^{-1} \text{ s}^{-1}$, and effective mixing.

Fluidized bed reactors

The applications of fluidized bed reactors have been extensively reported with around 1000 papers published on this topic over the past 6 years.^{32,64–74} Fluidized bed reactors are capable of utilizing an upward stream of fluid (gas or liquid) to allow particles in a stationary phase to be brought to a suspended or 'fluidized' state allowing for photocatalytic transformations to occur (Fig. (5)).

The advantages of this style of reactor include:

- low pressure drop,
- high throughput, and
- high photocatalyst surface area, which allows for increased catalyst–reactant interaction.

In 1992 Dibble and Raupp⁶⁶ used a flat plate fluidized bed reactor (Fig. (6)) to photooxidize trichloroethylene (TCE). A quantum efficiency range of 2–13% was achieved with a reaction rate peaking at $0.8 \mu\text{mol TCE (g catalyst)}^{-1} \text{ min}^{-1}$ [$2 \mu\text{mol (g TiO}_2\text{)}^{-1} \text{ min}^{-1}$]. These results are significant in that they are comparable with results produced in a liquid–solid slurry system for the oxidation of TCE; specifically demonstrating an order of magnitude increase. TCE is a standard evaluation test carried out by many, including more recently Lim and Kim who investigated a

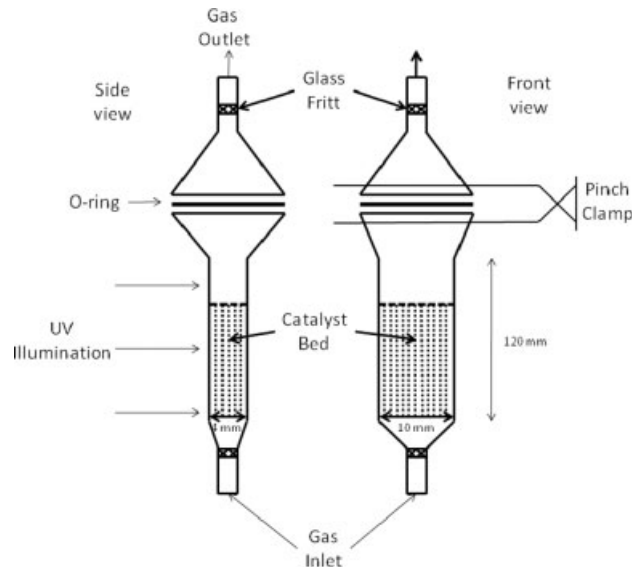


Figure 6. Schematic of flat plate fluidized bed reactor displaying the illumination direction and catalyst bed location. (Reproduced from reference 66 with permission from Elsevier)

circulated fluidized bed reactor (CFDB).⁶⁷ The design of this reactor utilised a loop seal which allowed particles that were carried up by the air stream to flow back down and re-enter the system. Several other factors were investigated in this paper including UV wavelength, initial TCE concentration, circulation rate, and O_2 and H_2O concentrations.

A two-dimensional fluidized bed reactor was used by Lim *et al.*⁷⁵ in the photocatalytic reaction of NO. Utilizing an annular flow-photoreactor the authors reported that this configuration enabled efficient contact between a P25 TiO_2 photocatalyst and the reactant gas (NO) which, when coupled with effective light transmission to the unit, facilitated the photocatalytic reaction. A series of altering conditions were assessed as a means to increase photocatalytic efficiency, including initial gas concentration, residence time of gas, reaction temperature, and irradiation intensity. A particular point of interest in this publication surrounded the superficial gas velocity and light transmission interaction. Results displayed in Fig. 7 show that increasing superficial gas velocity increased light transmission in the reactor. The light intensity significantly increased at approximately $1.3 U_{\text{mf}}$ (minimum fluidization velocity) which equated to a sharp increase in NO conversion. Below this value the UV light transmission through the catalyst bed was minimal. The photocatalytic conversion of NO continued to increase until U_{mf} reached 2.5, where a 70% conversion was achieved. Based upon their results Lim *et al.*⁷⁵ concluded that this process required adequate residence time and an effective gas velocity to produce bubbles of an appropriate size to ensure contact between UV light and the TiO_2 –NO system.

Son *et al.*⁷⁰ investigated the use of combined TiO_2 particles with Al_2O_3 in an attempt to overcome the drawbacks associated with fluidized reactors for photocatalysis. Paz⁶⁵ reported that fluidization of small particles such as P-25 was challenging due to 'drifting' from the primary operation area in the unit. Combining the catalyst, however, with larger particles such as Al_2O_3 could eliminate this problem and as such many researchers use an Al– TiO_2 catalyst. Son⁷⁰ focused on the decomposition of acetic acid and ammonia utilizing a three-phase photocatalytic system.

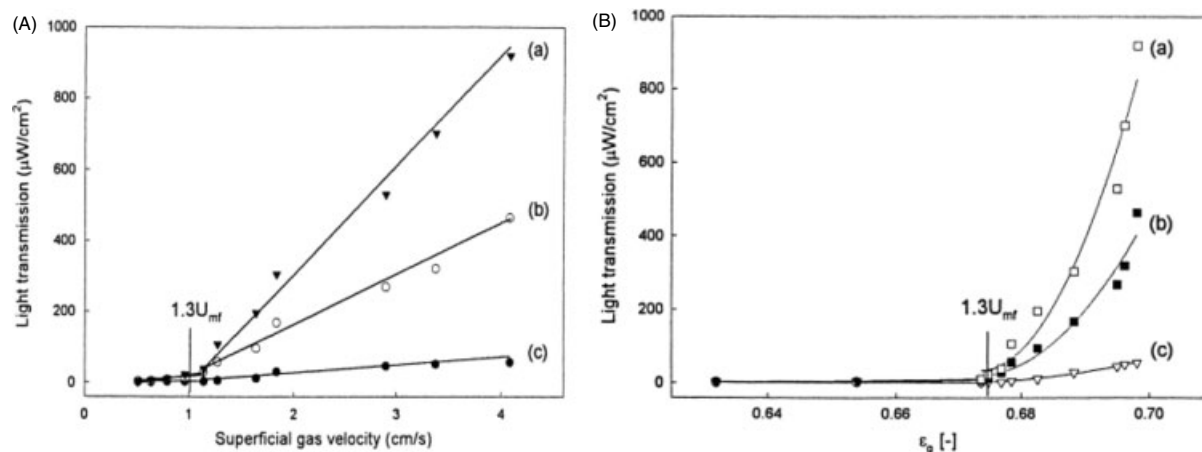


Figure 7. Results observed for the effect of (A) superficial gas velocity and (B) voidage on light transmission with measuring light at (a) 96 mm, (b) 53 mm and (c) 10 mm. (Reproduced from reference 75 with permission from Elsevier)

Decomposition was enhanced when carried out in the three-phase fluidized bed reactor, with significant improvement over use in a steady reactor. Production of N_2 and CO_2 were monitored as a means of measuring acetic acid and ammonia decomposition. In terms of acetic acid decomposition the fluidized bed showed increased efficiency over that of a conventional steady reactor along with increased efficiency with the addition of Al-TiO₂ instead of solely TiO₂; the conversion of acetic acid to CO_2 reached approximately 90% after 600 min with 10 mol% Al-TiO₂. A similar trend was observed for ammonia decomposition, with a conversion rate >95% being reached with 10 mol% Al-TiO₂ compared with 70% in the steady reactor. A point of interest is the suppression of the more undesirable products i.e. NO_2 and NO_3 with the use of Al-TiO₂ when compared with increased levels with pure TiO₂. In a previous study that used a FeTiO₂ material it was reported that the anatase structure of the catalyst transformed into a rutile structure after methanol destruction.⁷¹ Son *et al.*,⁷⁰ however, found that replacing the Fe with Al produces a catalyst with increased stability, thus providing enhancing ammonia decomposition. They concluded from their results that the efficiency of removal of VOC is increased by both the use of Al-TiO₂ combined particles and a fluidized reactor.

Nelson *et al.*⁷² reported the comparison of a fluidized TiO₂ system for methanol oxidation with a packed bed reactor. They concluded that fluidization resulted in faster rates of photocatalytic decomposition than achieved on the packed bed unit. A rate of $2.0 \times 10^{-7} \text{ mol cm}^{-3} \text{ min}^{-1}$ for CO_2 production was achieved for the fluidized reactor compared with a CO_2 production rate of $1.0 \times 10^{-7} \text{ mol cm}^{-3} \text{ min}^{-1}$ obtained with the packed bed reactor. It was reported that the use of both static mixing and vibration in the process to reduce photocatalyst separation rates was, however, only effective with Degussa P25 and not TiO₂-Al₂O₃. Overall TiO₂-Al₂O₃ was found to be an effective photocatalyst which is in agreement with the results obtained by Paz.⁶⁵

The drawbacks of fluidizing pure TiO₂ has led to an increased number of papers reporting results using combined catalyst, demonstrated by Kuo *et al.*³² who investigated the removal of toluene vapours from a continuous gas stream. The specific limitations included the 'loss or trapping' of powder within a photoreactor due to the fine structure of TiO₂. These problems can often result in the powdered catalyst 'drifting' away from the main area of operation. The investigation used activated carbon

(AC) particles with a TiO₂ coating to overcome any fluidization problem and to promote an evenly distributed catalyst. The research investigated the impact of altered relative humidity (RH), varied TiO₂ loading weights, and the use of glass beads (GB) to replace AC along with and without the use of a reflector. The use of activated carbon solely is effective in the removal of toluene, however, upon saturation of the AC particles toluene removal decreased significantly. It was established that 30% RH was optimal for efficient toluene removal. Interestingly increasing RH did not result in increased rates of toluene removal suggesting there is competitive adsorption between water and toluene molecules at higher levels of RH. The degradation of toluene vapours was accredited to both the use of activated carbon and photocatalysis, however, saturation resulted in certain restrictions when solely using AC. The results showed that the combination of AC removal of toluene and the photocatalytic removal could significantly extend toluene removal duration. In comparing the effectiveness of the two catalyst types it was found that the GB/TiO₂ was half as effective as AC/TiO₂ catalyst for toluene removal.

Voronstov *et al.*⁷⁴ also investigated the use of vibration to improve fluidization of granular photocatalysts for the decomposition of gaseous acetone. A variety of fixed bed constructions were investigated together with the vibrofluidized bed system to enable efficient comparison. The vibrofluidized bed system was the most effective with an 8.7% increase in quantum efficiency being achieved. The high efficiency of the vibrofluidized bed was, interestingly, attributed to the external vibrations used together with the 'periodic light phenomenon'. This phenomenon resulted from the eccentric photocatalyst movement within the reactor which consequently enabled increased absorption of scattered light.

A fluidized bed system utilizing an upward stream of air which brought TiO₂ pellets to a fluidized state has also been reported.⁷⁶ The reactor consisted of a reaction chamber which contained a foraminated member supporting a bed of mobile photocatalysts along with an aeration device to allow for agitation of photocatalytic particles. The aeration device generated gas bubbles through a perforated shelf allowing agitation of photocatalysts. The reactor configuration was utilized for the treatment of waste water in a flow through style process. The reactor concept was designed to reduce or completely remove the need for moving parts, thus allowing for a reactor concept

with a reduced foot print suggesting a more energy efficient design. To ensure constant agitation of the particles the terminal settling velocity of the particles must not exceed the velocity of any upward flow of the liquid through the perforated shelf by more than 10 ms. The reactor retained the advantage of the use of pellets which both allow for reduced downstream processing and, via agitation, present a number of faces capable of excitation by illumination.

Immobilized liquid reactors

Fixed bed

Al-Ekabi and Serpone⁷⁷ investigated TiO₂ supported on a glass matrix for the photo-decomposition of phenol, 4-chlorophenol, 2,4-dichlorophenol, and 2,4,5-trichlorophenol. The degradation followed first-order kinetics with the reaction occurring on the surface of the semiconductor. The irradiation source was an AM-1 filter simulating solar irradiation. A fixed bed reactor system employing a fibre-optic cable (OFR) was reported by Pill and Hoffmann.³⁴ The system was conceived to allow for remote light distribution to photocatalysts, to effectively determine quantum yields through effective light flux measurement. Furthermore OFR allowed for reactor reuse to assess different coatings and light input angles, and to minimize potential heating and photocatalyst delamination. They anchored TiO₂ particles onto quartz fibres and light was transmitted to the TiO₂ particles via radial refraction of light out of the fibre. A maximum quantum efficiency of $\phi = 0.011$ for the oxidation of 4-chlorophenol was achieved. This can be compared to a maximum quantum efficiency of $\phi = 0.0065$ for 4-chlorophenol oxidation in a TiO₂ slurry reactor.

This study was followed with an investigation into the application of the OFR system to the photocatalytic degradation of pentachlorophenol, oxalate and dichloroacetate.³⁴ Relatively high apparent quantum efficiencies of $\phi = 0.010$, 0.17, and 0.08 were achieved for PCP, OX and DCA, respectively, with complete mineralization reported. It was concluded that the OFR system had the advantages of a fixed-bed unit together with the kinetic efficiency of a slurry reactor. The OFR configuration enhanced not only the distribution but also the uniformity of activated photocatalyst within a particular reaction volume compared to standard fixed-bed designs. These characteristics reduced mass transport limitations for photochemical conversion efficiency and allowed higher processing capacities. Furthermore, potential light loss via absorption or scattering by the reaction medium was minimized. The OFR system could be used in batch or continuous flow operation for both liquid and or gas phase reactions. The transmission cable also allowed for remote light delivery to the photocatalyst.

Nogueira and Jardim⁷⁸ reported the photodegradation of methylene blue using solar irradiation on a fixed bed reactor with TiO₂ immobilized on a flat glass plate as a support. They investigated the slope of the plate and found that methylene blue photodegradation was influenced by two factors:

- the fluid thickness film which flowed over the plate; and
- the light intensity that reached the system.

They reported a limited range of slopes 22–25° and found that 95.8% of the model compound was degraded at 22° slope while 89% was degraded at 25° angle. Ray and Beenackers⁷⁹ proposed a distributive type fixed bed reactor system that employed hollow glass tubes as light conductors for distribution to photocatalyst particles. The reactor configuration increased the surface to

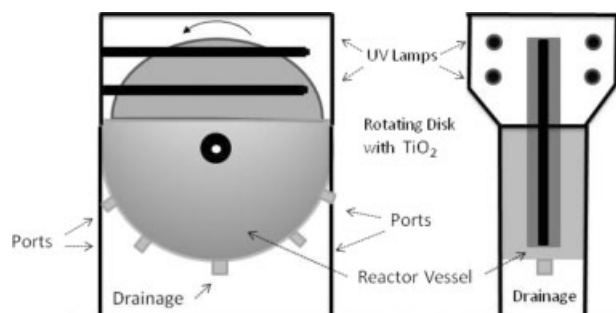


Figure 8. Schematic representation of rotating disc photo reactor. (Reproduced from reference 81 with permission from Elsevier)

volume ratio while eliminating the potential light loss through absorption and scattering by reaction matrix. This configuration enabled a large surface of photocatalyst to be deployed within a relatively small reactor volume. Between 70 and 100 fold increase in surface area per m³ of reactor volume was achieved compared with a conventional annular reactor configuration. The photo-degradation of special brilliant blue, a model dye pollutant, was investigated and 90% photocatalytic destruction of the dye achieved after 100 min irradiation. This study was followed up with the development of a tube light reactor which had a 100–150-fold increase in surface area per unit volume of fluid being treated compared to a conventional annular reactor design and a 10–20-fold increase over an immersion reactor. In a study of a reactor volume of 3.65×10^{-4} m³ containing 21 U-shaped lamps of diameter 0.45 cm coated with the P25 photocatalyst, a 695% increase in reactor efficiency was achieved compared with an annular photocatalytic reactor. Furthermore a 259% increase in efficiency was obtained for the new unit compared with a slurry reactor.

Feitz *et al.*⁸⁰ investigated two fixed bed photocatalytic reactors, a packed bed reactor and a coated mesh reactor, using solar illumination. They assessed the processing rate for 2 mg L⁻¹ phenol solutions, and calculated a rate of 140 mg m⁻² h⁻¹ for the packed bed reactor with a rate of 20 mg m⁻² h⁻¹ for the coated mesh reactor. The lower activity obtained with the coated mesh reactor was believed to be due to insufficient photocatalyst surface contact, low levels of available attached TiO₂, and a small reactor to tank volume ratio. Photonic efficiencies for the decomposition of 100 mg⁻¹ dichloroacetic acid solutions using the packed bed unit were only 40% lower than suspension systems. They therefore proposed that this system was particularly effective for treating contaminated water.

Dionysiou *et al.*⁸¹ developed a TiO₂ rotating disk reactor for the decomposition of organic pollutants in water (Fig. (8)). They used a commercial TiO₂ composite ceramic ball photocatalyst material. LiCl tracer studies performed under different disk angular velocities, between 5 and 20 rpm, demonstrated that mixing in the rotating disk photocatalytic reactor RDPR was similar to that of a continuous stirred tank reactor. They reported the destruction of >90% 4-chlorobenzoic acid after 6 h irradiation. The light intensity distribution within the reactor was also determined and found to vary from about 30 to 1500 μ W cm⁻² within the reactor. The RDPR has a number of advantages: it eliminates the need for effluent filtration as the catalyst is immobilized, the 3-D nature of the flow created enables effective mixing, while the formation of the thin film allows more effective oxygen transport from the gas phase to the photocatalyst surface. The photonic efficiency

calculated for the experiment at 4 rpm was 2.7%. The authors anticipate this value to improve with process optimization.^{82,82} A similar study by Hamill *et al.*⁸³ reported the use of a sealed rotating photocatalytic reactor (RPC) of similar configuration to the Dionysiou RDPR.^{81,82,84} They investigated the photo-degradation of dichlorobutene and examined the effects of mass transfer and combinations of pollutants. They reported that the RPC could effectively degrade a range of substrates and that the degradation rate was dependent on rotation speed. They also reported that this configuration could be applied to both volatile and non-volatile pollutants.

Mehrvar *et al.*²⁷ reported the use of a photoreactor with TiO₂ coated tellerette packing. The tellerette packings were constructed from stainless steel welding wire which was 'roughened' to promote the adhesion of TiO₂ to the surface. The wires were then wound in a spiral or 'spring like' structure to be formed. The wound wire was cut into smaller lengths and each individual 'spring' adjusted to allow the ends to be brought together to form the tellerette shape. The tellerette type packings were selected and manufactured on the basis that they would permit sufficient light dispersion into the interior of the bed to maintain effective photocatalytic reaction rates with no significant mass transfer limitations. The photoreactor allowed substantial UV light penetration throughout its interior, and had no significant mass transfer limitations during the photocatalytic degradation of 1,2-dioxane. It was concluded that at the range of attenuation coefficients of interest, the reaction rate at various radial positions would not be significantly mass transfer limited unless the photocatalyst activity was increased by at least one order of magnitude.

A novel photocatalytic reaction system, composed of solution and gas spaces that were divided by a thin Teflon film and TiO₂ coated mesh or cloth has been reported.⁸⁵ The activity of TiO₂ immobilized on a stainless steel mesh and on a fibre-glass cloth using isopropanol as a model compound was investigated. Although both support materials yielded comparable photocatalytic activities the fibre glass cloth was the most stable. The Teflon membrane enhanced the O₂ levels in the reaction solution, which increased the photocatalytic activity for the destruction of organic compounds in water. The benefit of this system for the photo-degradation of aqueous volatile organic carbons was that it did not require air bubbling, which resulted in volatilization of the contaminants to the atmosphere.

Lim *et al.*⁶⁸ reported the use of an external lamp, annular photocatalytic reactor with TiO₂ adsorbed on a quartz tube for the degradation of phenanthrene and pyrene from a dilute water stream. They reported that above a feed velocity of 7 cm min⁻¹ the process was rate controlled and not influenced by mass transfer limitations.

A tubular photocatalytic reactor for water purification using a ceramic cylindrical tube with a Pt-loaded TiO₂ film coated on the inner surface of the tube has been developed by Zhang *et al.*⁸⁶ Phenol, trichloroethylene, and bisphenol A were used as model pollutants to examine the effectiveness of the photoreactor. The complete degradation of each pollutant within 2 h reaction time was observed, with the authors concluding that the performance of the reactor was dependent on the aeration of the system.

McMurray *et al.*⁸⁷ reported the use of a stirred tank reactor with immobilized Degussa P25 TiO₂ for the degradation of oxalic acid and formic acid. The rate of degradation of both acids was not mass transfer limited with propeller speeds greater than 1000 rpm.

They reported apparent quantum yields of 5% for oxalic acid and 10% for formic acid.

A sol-gel prepared TiO₂ coating on a tubular photocatalytic reactor with re-circulation mode and a batch photocatalytic reactor was investigated by Lin *et al.*⁸⁸ for the degradation of methylene blue and phenol. The sol-gel film synthesised demonstrated effective photocatalytic activity for the decomposition of organic compounds in water and the authors proposed the use of this reactor for water purification. During a 180 min photoreaction of phenanthrene, 67.6% destruction was observed with 40.1% conversion to CO₂.

Zhang *et al.*³⁸ reported the use of a corrugated plate reactor configuration which was developed and assessed using 4-chlorophenol as model pollutant. They compared the new configuration with a flat plate reactor and a slurry reactor. The corrugated plate reactor was reported to be 150% faster with mass transfer rates 600% higher than that of a flat plate reactor. The authors suggested that the enhanced performance of the corrugated configuration was a result of the relatively larger illuminated photocatalyst surface area per unit volume, coupled with effective delivery of both photons and reactants to the photocatalyst surface.

The photocatalytic oxidation of a non-ionic surfactant was carried out in a labyrinth flow reactor with an immobilized photocatalyst bed.⁸⁹ The work focused on the effects of flow-rate on the decomposition of the non-ionic surfactant. The authors concluded that the optimum photodegradation of the surfactant was observed with a flow-rate of 11.98 dm³ h⁻¹. They further studied the remediation of Acid Red 18, an azo dye.⁹⁰ Long reaction times were investigated for the photodegradation of Acid Red using an immobilized Aeroxide Degussa P25 catalyst. Slower flow rates affected the efficiency of the system, with mineralization times varying from 35 h to 60 h depending on flow rate.

An annular photocatalytic reactor, assimilated to a plug flow reactor, with a fixed bed of Degussa P25 immobilized onto a fibre glass support was reported for the remediation of gaseous acetone²⁶ (Fig. (9)). There was no limitation on mass transfer observed either internally or externally under the experimental conditions investigated.

An internally illuminated monolith reactor (IIMR) has been reported in the investigation of multi-phase photocatalysis.^{91,92} The IIMR had side light emitting fibres incorporated within the channels of a ceramic monolith containing TiO₂ photocatalyst coated individual channel walls. Photonic efficiencies obtained with this reactor were below those obtained for a slurry reactor but greater than that reported for an annular photoreactor and a reactor configuration with side light fibres immersed in a TiO₂ slurry. The authors reported that the IIMR had a larger area of catalyst exposed to illumination and this is its key advantage over other photocatalytic reactors.

Immobilized gas reactors

The use of the Optical Fibre Reactor (OFR) for the photoreduction of CO₂ to fuels by a visible light activated catalyst has been reported by Nguyen and Wu.⁹³ The optical fibres were coated with a gel-derived TiO₂-SiO₂ mixed photocatalyst. The OFR reactor operated on the principle of incident light being split in two beams when first in contact with the surface of the fibre (Fig. 10). Part of the light penetrates the layer of catalyst on the fibre and creates excitation, while the other beam is reflected off the fibre and transmitted along the length of the optical fibre. This allowed the light to gradually spread through the

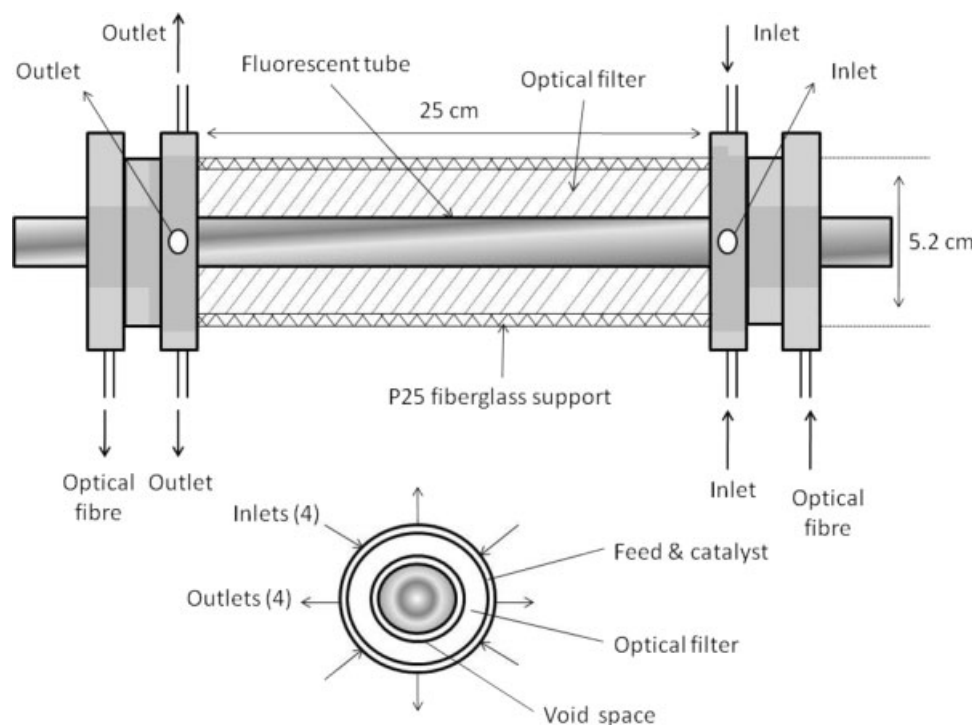


Figure 9. Schematic representation (A) and sectional drawing (B) of the annular photoreactor. (Reproduced from reference 26 with permission from Elsevier)

length of the reactor. Two photocatalysts were utilized in this investigation; Cu–Fe/TiO₂ and Cu–Fe/TiO₂–SiO₂. The products obtained in this study included ethylene and methane, along with traces of ethane and methanol. The product formation under UVA illumination demonstrated selectivity towards the photocatalyst used, with the exception of methane, which was evolved with each of the photocatalysts. The highest rate of methane production, 1.860 $\mu\text{mol g}^{-1}\text{-cat h}^{-1}$ was found when the catalyst Cu(0.5%(w/w))–Fe(0.5%(w/w))/TiO₂–SiO₂–acetyl acetone (acac) was used. Ethylene evolution was selective in production and was only seen over Fe- and Cu-containing catalysts; the highest production rate of 0.575 $\mu\text{mol g}^{-1}\text{ h}^{-1}$ was found when the catalyst Cu(0.5%(w/w))–Fe(0.5%(w/w))/TiO₂ on optical fibres was used. In comparison, natural sunlight (from a solar concentrator) produced a production rate of 0.279 $\mu\text{mol g}^{-1}\text{ h}^{-1}$ with the catalyst Cu(0.5%(w/w))–Fe(0.5%(w/w))/TiO₂–SiO₂–acac, significantly higher than the rate for the TiO₂–SiO₂ catalyst. These results were attributed to the increased surface area from the use of TiO₂–SiO₂ in comparison with pure TiO₂ and the presence of Cu and Fe metals which shifted the light absorption into the visible spectrum. The benefits of this system included uniform light distribution throughout the reactor, a feature not seen in traditional packed bed designs, and the visible light driven catalyst, which the authors concluded enhanced applicability at commercial and industrial scales.

Immobilized vapour reactors

The development of a cost effective and easy-to-use catalyst support for an immobilized system was investigated by Haijiesmaili *et al.*⁹⁴ This investigation focused on TiO₂ supported on a three-dimensional carbon foam for the oxidation of gaseous methanol in a vapour phase flow-through photoreactor. An impregnation technique was adopted for production of the

TiO₂ supported carbon foam; carbon foam was immersed in a TiO₂ (P25)–water/ethanol (1 : 1) solution followed by drying. The photoreactor was established by packing the carbon foam supported TiO₂ into a Pyrex tube with internal illumination from an 8 W central UV-A light. Results were based upon methanol conversion and CO₂ and formaldehyde selectivity. The methanol conversion with the carbon foam supported TiO₂ was dependent on TiO₂ loading where TiO₂ loadings of 7.7, 9.4, 16.3 and 28.5%(w/w) achieved methanol conversions of 52, 57, 61 and 75%, respectively. A maximum methanol conversion of 81% was achieved for a 666%(w/w) TiO₂ loading. These results were impressive compared with those obtained in a photoreactor where the TiO₂ photocatalyst was simply coated on the inside of the reactor wall. In this case the highest methanol conversion reached was 22%, whereafter any increase in TiO₂ loading resulted in a screening effect of excess particles, resulting in no further increase in methanol conversion. CO₂ and formaldehyde selectivity further supported the findings in the paper with CO₂ reaching 44%, compared with 7% for a wall coated reactor. The efficiency of the carbon foam supported TiO₂ photoreactor was attributed to the ability to increase the exposed surface of the carbon foam and hence increase the surface to reactor ratio, which allowed increased TiO₂ content within the reactor. The authors concluded that the reactors air to surface ratio and its ability to perform at very low pressure drops allow its use in practical applications.

Suspension vs. immobilized reactors: a comparison

Dutta and Ray²⁸ developed a Taylor vortex photocatalytic reactor that created unsteady Taylor–Couette flow between two co-axial cylinders through re-circulation of fluids from the body of the reactor to the inner cylinder wall, coated with TiO₂ (Fig. 11(a) and (b)). The Taylor–Couette flow is the movement of viscous fluids in between a pair of coaxial cylinders which experience

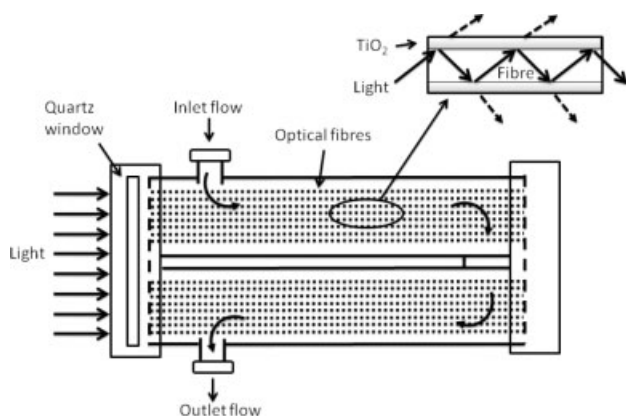


Figure 10. Schematic of optical fibre photo reactor displaying light transmission along coated fibres. (Reproduced from reference 93 with permission from Elsevier)

inner centrifugal instability when the inner cylinder rotates differentially with respect to the outer cylinder. They investigated the effect of Reynolds number (Fig. 11(c)) and catalyst loading on photodegradation and compared the results with that for a slurry reactor. They noted that increasing the Reynolds number increased the rate of photodegradation of their model pollutant orange II, demonstrating that external mass transfer controlled the overall reaction rate.

The performance of a suspended catalyst system, an immobilized catalyst where the wall of the reactor was coated, and an immobilized system packed with coated glass beads have been compared for the photodegradation of formic acid.⁹⁵ Mass transfer limitations were observed in the immobilized system with the catalyst coated on the reactor wall. However aerating the system overcame this mass transfer problem. The performance of the packed bed reactor was investigated for two different sized beads ($d = 1.3$ and 2 mm) to gain an understanding of the photocatalytic activity. The authors concluded that large beads enhanced the photocatalytic activity.

A pilot reactor utilizing a TiO_2 coated 15 pores-per-inch alumina reticulated foam monolith incorporated in the space between a centrally deployed UV lamp and the internal wall of the reactor was compared with a Degussa P25 TiO_2 slurry system.⁹⁶ Results for the degradation of 1,8-diazobicyclo[5.4.0]undec-7-ene (DBU) indicated that the foam monolith immobilized photocatalyst system was more efficient than the slurry photocatalyst reactor suggesting that the immobilized system could be scaled up for water purification.

Three different reactor configurations, slurry reactor, wall reactor, and fixed-bed reactor, were compared for the photocatalytic disinfection of *Escherichia coli* aqueous suspensions and methylene blue photodegradation (Fig. 12). Titania was in suspension for the slurry reactor, immobilized on the reactor wall for the wall reactor, and immobilized on the packing in the fixed bed reactor.⁹⁷ The authors investigated the effect of increasing catalyst layer thickness and compared it with increasing concentration of catalyst in the slurry system. The results for methylene blue photo-oxidation were in good agreement for both slurry and immobilized system. For the photocatalytic disinfection, however, this was not the case. The increased density of TiO_2 film caused by the heat treatment reduced the surface area of catalyst available for the micro-organisms and therefore reduced the photocatalytic activity. When the immobilized reactor was investigated for efflu-

ents sampled from a wastewater treatment plant, however, they required comparable irradiation times to the slurry system to reach the bacterial detection limit.

Industrial applications

The potential industrial applications for semiconductor photocatalysis are wide and diverse ranging from treating oil and gas effluent to potable water. The reality of research based photoreactor designs are, however, that very few laboratory scale test reactors are ultimately feasible in terms of industrial scale up. In an industrial environment the volume and rate of waste effluent production is in the order of hundreds of cubic meters, i.e. millions of litres per day. Typically laboratory photoreactors have a capacity of between 1 mL and 1 L, with a UV illumination source between 36 W and 500 W. Transforming a 1 L capacity reactor to a 1 m^3 capacity unit is not a simple transformation, with the relationship between materials, volume, catalyst loading, turbidity, and UV penetration presenting complex challenges.

Examples where industrial scale photoreactors have been employed on a large scale are those of solar activated designs. Solar photoreactors have the advantage of not requiring artificial light sources but do require huge amounts of space and also depend on the solar insolation.^{98–100}

Pilot scale studies

Imoberdorf *et al.*¹⁰¹ proposed a scaled up multi-annular photocatalytic reactor for the remediation of air pollution. This consisted of four concentric cylindrical borosilicate glass tubes (Fig. 13). The illumination source, a Philips TL18W UV lamp, was placed on the central axis of the system. With the available reaction length of 177 cm the total surface area available for radical production was 5209 cm^2 , a significant increase on the 81 cm^2 of the laboratory test reactor. Using a sol-gel process a thin layer of TiO_2 was coated on two walls of the reactor, which were in contact with the gas flowing through each annulus of the unit.

In this study Imoberdorf *et al.*¹⁰¹ examined the mechanisms of radiative transfer, rate kinetics, and mass transfer. They proposed that the process should be free from mass transfer limitations with a reactor operated under kinetic control. It was found that it was possible to make accurate predictions of reactor behaviour, based purely on the chemical reaction fundamentals, reactor engineering, and radiation transport theory. This took no account of the adjustable or unknown parameters of photoreactor design.

Shu and Chang¹⁰² reported the investigation of a pilot scale thin gap annular plug flow (TGAPF) and photoreactor and recirculated batch reactor for the degradation of azo dye waste water using H_2O_2 instead of a semiconductor photocatalyst. The TGAPF system was tested using acid orange 10 at a concentration of 20 mg L^{-1} with a simulated waste water prepared in a tank reservoir with a total volume of 100 L. The TGAPF reactor had a capacity of 3000 mL and the dye was pumped through at a rate of 1.5 L min^{-1} to 6.5 L min^{-1} , which gave a throughput of $2.35\text{--}9.32 \text{ m}^3 \text{ day}^{-1}$. The UV lamp source was a 5000 W medium pressure mercury lamp at 253.7 nm and was positioned centrally in the quartz housing. This configuration achieved a degradation rate of 0.26 min per L of dye to 99% of original concentration, e.g. 100 L in 26.9 min. When compared with the degradation rate of the recirculated batch reactor the TGAPF reactor was 233 times more efficient, with the batch reactor taking 6267 min to degrade the same volume and concentration of azo dye.

These two examples of scaled up pilot photoreactors show that there is the potential for increasing capacity, although it

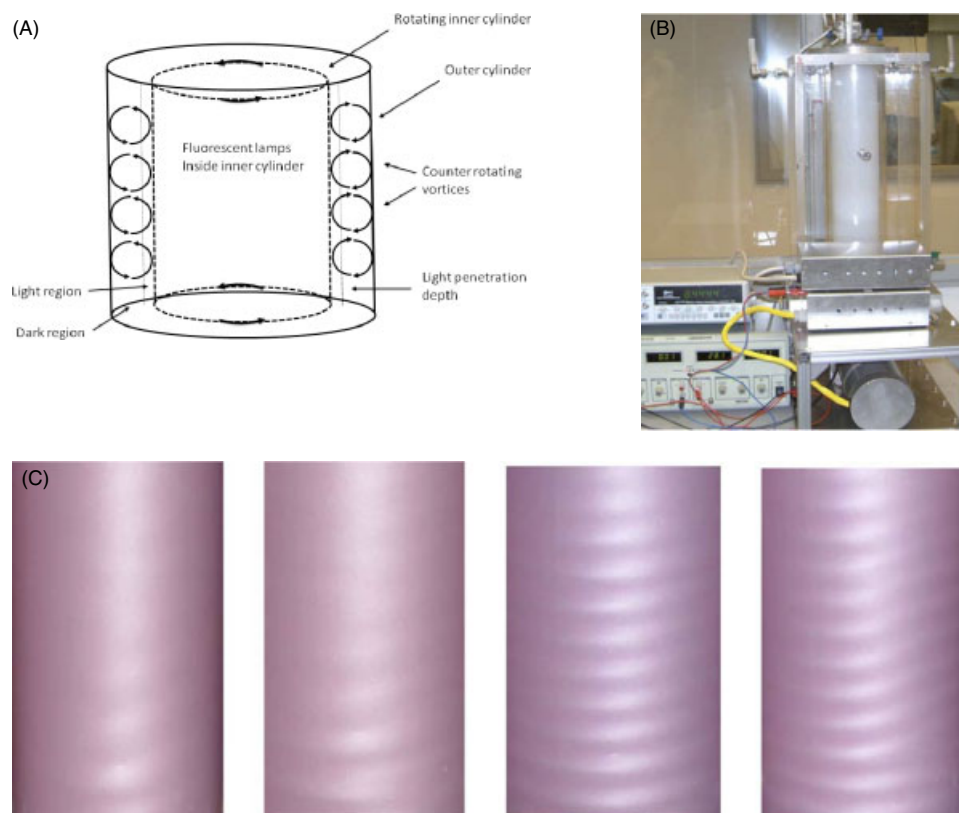


Figure 11. (A) Schematic of Taylor vortex reactor and (B) image of Taylor vortex photocatalytic reactor. (C) Progress of time-dependent Taylor vortex flow around critical Reynolds number, $Re_c = 111$. (Reproduced from references 28 and 29 with permission from Elsevier)

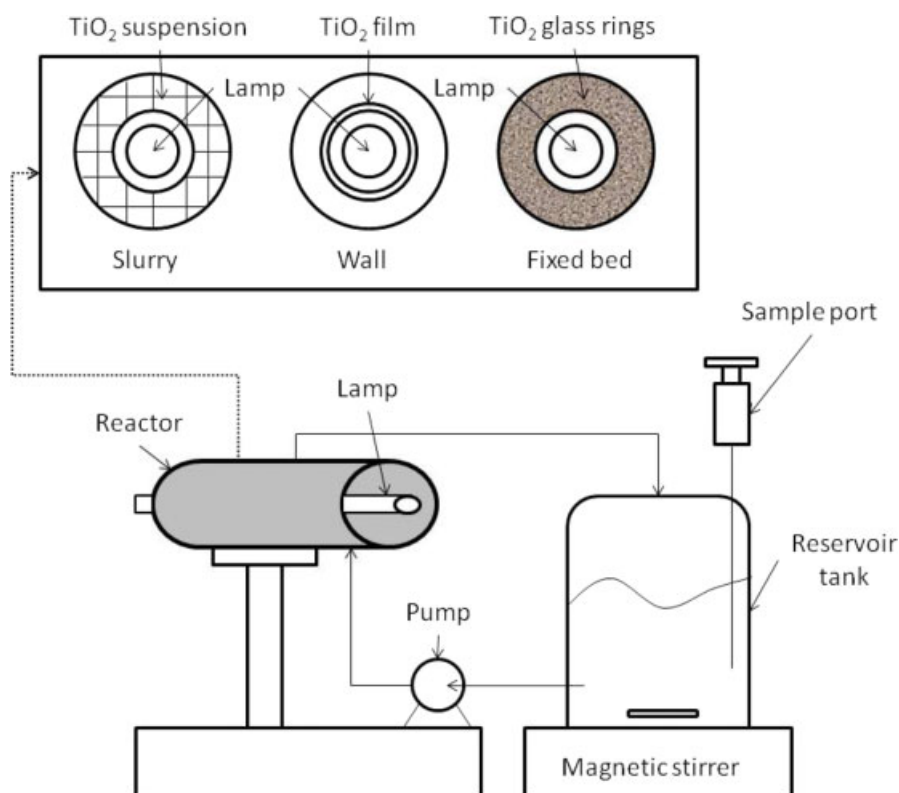


Figure 12. (A) A slurry reactor, using suspensions of Degussa P25 TiO₂. (B) A wall reactor, immobilizing Degussa P25 TiO₂ onto the 15 cm long glass tube that constitutes the inner-tube wall of the reactor. (C) A fixed-bed reactor, immobilizing Degussa P25 TiO₂ onto 6 mm × 6 mm glass Raschig rings placed into the annular reactor volume. (Reproduced from reference 97 with permission from Elsevier)

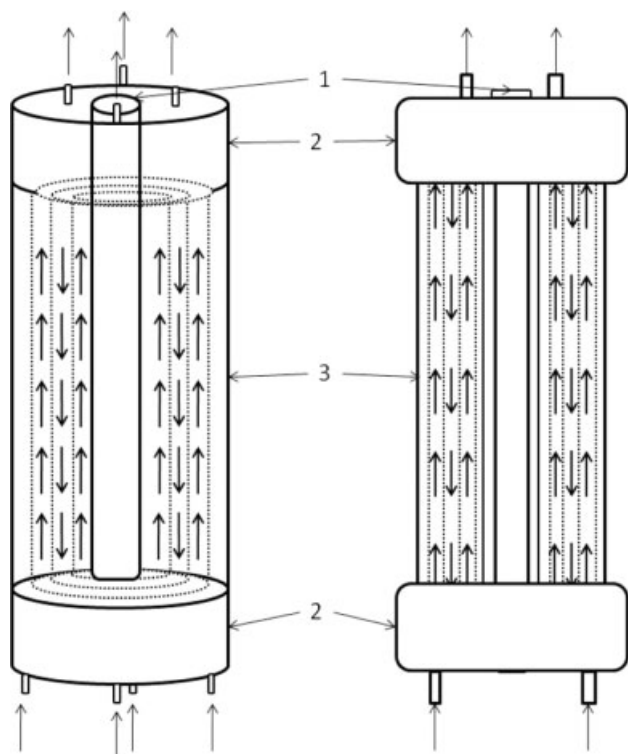


Figure 13. Schematic representation of a pilot-scale multi-annular photocatalytic reactor: (A) UV lamp, (B) distribution heads, and (C) borosilicate glass tubes. (Reproduced from reference 101 with permission from Elsevier)

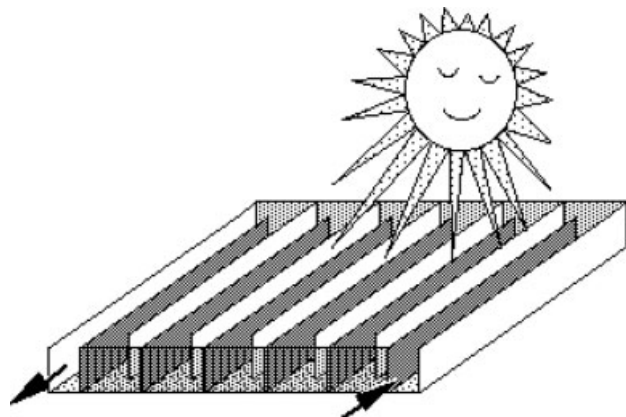


Figure 14. Schematic view of a DSSR reactor showing the inner structure of the transparent structured box made of PLEXIGLAS[®] (reproduced from Reference 103 with permission from ASME).

is worth noting that the Shu and Chang TGAPF reactor does require a 5000 W UV source which is expensive and has significant associated operating costs.

The double skin sheet reactor (DSSR) comprises a flat transparent box framework constructed from PLEXIGLAS[®] (Fig. 14). The photocatalyst was deployed as a suspension in the waste water and the slurry was then pumped through the channels of the unit. After the degradation process the photocatalyst had to be removed from the suspension either by filtering or by sedimentation. The DSSR has been demonstrated to utilize both the direct and the diffuse portion of solar radiation. A pilot scale DSSR, has been investigated for the treatment of industrial wastewater effluent in

Wolfsburg, Germany.¹⁰⁰ 50% of the organic pollutants in the waste water were degraded within 8–11 h irradiation. The efficiency of the photocatalytic process was found to be dependent on the initial pollutant concentration, the time of illumination, and, not surprisingly, the solar UV light flux density.

CONCLUSIONS

The research detailed in this review highlights the diversity in photocatalytic reactor design along with their potential applications. Suspended liquid reactors, immobilized liquid reactors, immobilized gas reactors and immobilized vapour reactors were considered and, where appropriate, compared in an attempt to address the advantages and disadvantages of individual designs.

The following conclusions could be drawn following a consideration of the current state of the art in this field.

1. Slurry and suspended systems offer the advantage of increased surface area allowing increased photocatalyst and reactant interaction and has proved effective in the treatment of wastewater. Limited light penetration and downstream processing procedures, particularly with respect to catalyst separation, however, restrict these concepts for commercialization and scale up.
2. Fluidized bed reactors also present excellent photocatalyst surface area to pollutant ratios for photocatalytic transformations. Research has demonstrated that these systems are effective for both gas and liquid phase photocatalysis. This has enabled the use of highly efficient powders such as Degussa P25, which benefit from the 'periodic light phenomenon' created by fluidized systems. Drawbacks to the system include the loss or 'drifting' of particles within the system and downstream processing restrictions.
3. Fixed bed designs utilize immobilized catalysts which have the advantages of no downstream processing restrictions such as separation and filtration and allow operation in both batch and continuous flow phase. There are restrictions regarding this system including difficulty in the illumination of the entire support containing the catalyst and mass transfer limitations affected by catalyst thickness. Furthermore, in order to achieve an effective surface area of photocatalyst relative to the effluent being treated, scaled up units require a significant 'footprint'.
4. Comparisons of the systems demonstrate that given the correct parameters the individual concepts are effective. While many comparisons of systems describe the immobilized catalyst reactor set-up as having decreased efficiency or restrictions due to mass transfer limitations, it was reported that if such restrictions were overcome results were comparable with those of slurry and fluidization systems.

As has been demonstrated here, a vast array of photoreactor concepts have been reported, all displaying varying engineering characteristics in terms of efficiency for pollutant transport, photocatalyst deployment, and activation. These characteristics are all critical, however, the future of photoreactor technology does not solely rely in the design of the reactor itself, but in the development of more effective photocatalysts, particularly in rate limited systems. The development of photocatalysts that can achieve greater conversion efficiencies at lower irradiation energies, and ultimately visible light absorbing materials will be a critical component in ensuring wide scale adoption of this versatile technology. For industrial applications photoreactors need to meet the challenge of capacity, ruggedness, reliability and

ease of use. Currently the only design of photoreactor which is capable of processing the level of wastewater required is that of suspension reactors, but as noted in this review they are far from infallible. Ultimately, however, the application of semiconductor photocatalysis for remediation has real scope for impacting on water pollution and hence global water scarcity.

ACKNOWLEDGEMENTS

The Authors would like to thank the Scottish Funding Council for funding Cathy McCullagh's lectureship under the Northern Research Partnership research pool. The authors also gratefully acknowledge funding of the positions of Nathan Skillen and Morgan Adams by the Engineering and Physical Sciences Research Council.

REFERENCES

- Ollis DF and Al-Ekhabi H, *Photocatalytic Purification and Treatment of Water and Air*. Elsevier (1993).
- Mills A and LeHunte S, An overview of semiconductor photocatalysis. *J Photochem Photobiol A: Chem* **108**:1–35 (1997).
- Hoffman AJ, Carraway ER and Hoffmann MR, Photocatalytic production of H_2O_2 and organic peroxides on quantum-sized semiconductor colloids. *Environ Sci Technol* **28**:776–785 (1994).
- Fox MA and Dulay MT, Heterogeneous photocatalysis. *Chem Rev* **93**:341–357 (1993).
- Fujishima A, Rao TN and Tryk DA, Titanium dioxide photocatalysis. *J Photochem Photobiol C: Photochem Rev* **1**:1–21 (2000).
- Ireland JC, Klostermann P, Rice EW and Clark RM, Inactivation of *Escherichia coli* by titanium dioxide photocatalytic oxidation. *Appl Environ Microbiol* **59**:1668–1670 (1993).
- McCullagh C, Robertson J, Bahnemann D and Robertson P, The application of TiO_2 photocatalysis for disinfection of water contaminated with pathogenic micro-organisms: a review. *Res Chem Intermed* **33**:359–375 (2007).
- Sjogren JC and Sierka RA, Inactivation of phage ms2 by iron-aided titanium dioxide photocatalysis. *Appl Environ Microbiol* **60**:344–347 (1994).
- Cai R, Hashimoto K, Kubota Y and Fujishima A, Increment of photocatalytic killing of cancer cells using TiO_2 with the aid of superoxide dismutase. *Chem Lett* 427–430 (1992).
- Cai R, Kubota Y, Shuin T, Hashimoto K and Fujishima A, Induction of cytotoxicity by photo-excited TiO_2 particles. *Cancer Res* **52**:2346–2348 (1992).
- Fujishima A and Honda K, Electrochemical photolysis of water at a semiconductor electrode. *Nature* **238**:37–38 (1972).
- Karakitsou KE and Verekios XE, Effects of altermultivalent cation doping of titania on its performance as a photocatalyst for water cleavage. *J Phys Chem* **97**:1184–1189 (1993).
- Suzuki K, in *Photocatalytic Purification and Treatment of Water and Air*, ed by Ollis David F and Al-Ekhabi H. Elsevier (1993).
- Borgarello E, Kiwi J, Pelizzetti E, Visca M and Gratzel M, Photochemical cleavage of water by photocatalysis. *Nature* **289**:158–160 (1981).
- Taqi Khan MM and Nageswara Rao N, Stepwise reduction of coordinated dinitrogen to ammonia via diazido and hydrazido intermediates on a visible light irradiated $Pt/CdS \cdot Ag_2S/RuO_2$ particulate system suspended in an aqueous solution of $K[Ru(EDTA-H)Cl]2H_2O$. *J Photochem Photobiol A: Chem* **56**:101–111 (1991).
- Schiavello M, Some working principles of heterogeneous photocatalysis by semiconductors. *Electrochim Acta* **38**:11–14 (1993).
- Taqi Khan MM, Chatterjee D and Bala M, Photocatalytic reduction of N_2 to NH_3 sensitized by the $[Ru(II)\text{-}ethylenediaminetetraacetate\text{-}2,2'\text{-}bipyridyl]$ complex in a $Pt\text{-}TiO_2$ semiconductor particulate system. *J Photochem Photobiol A: Chem* **67**:349–352 (1992).
- Khan MMT, Chatterjee D, Krishnaratnam M and Bala M, Photosensitized reduction of N_2 by $Ru(bipy)_3^{2+}$ adsorbed on the surface of $Pt/TiO_2/RuO_2$ semiconductor particulate system containing $Ru(II)\text{-}EDTA$ complex and L-ascorbic acid. *J Mol Catal* **72**:13–18 (1992).
- Gerischer H and Heller A, Photocatalytic oxidation of organic molecules at titanium dioxide particles by sunlight in aerated water. *J Electrochem Soc* **139**:1992.
- Jackson NB, Wang CM, Luo Z, Schwitzgebel J, Ekerdt JG and Brock JR, et al, Attachment of TiO_2 powders to hollow glass microbeads: activity of the TiO_2 -coated beads in the photoassisted oxidation of ethanol to acetaldehyde. *J Electrochem Soc* **138**:3660–3664 (1992).
- Nair M, Luo Z and Heller A, Rates of photocatalytic oxidation of crude oil on salt water on buoyant, cenosphere-attached titanium dioxide. *Ind Eng Chem Res* **32**:2318–2323 (1993).
- Boer KW, *Survey of Semiconductor Physics*. Van Nostrand, New York (1990).
- Kormann C, Bahnemann DW and Hoffmann MR, Photocatalytic production of hydrogen peroxides and organic peroxides in aqueous suspensions of titanium dioxide, zinc oxide, and desert sand. *Environ Sci Technol* **22**:798–806 (1988).
- Carraway ER, Hoffman AJ and Hoffmann MR, Photocatalytic oxidation of organic acids on quantum-sized semiconductor colloids. *Environ Sci Technol* **28**:786–793 (1994).
- Mohseni M, Gas phase trichloroethylene (TCE) photooxidation and byproduct formation: photolysis vs. titania/silica based photocatalysis. *Chemosphere* **59**:335–342 (2005).
- Vincent G, Marquaire PM and Zahraa O, Abatement of volatile organic compounds using an annular photocatalytic reactor: study of gaseous acetone. *J Photochem Photobiol A: Chem* **197**:177–189 (2008).
- Mehrvar M, Anderson WA and Moo-Young M, Preliminary analysis of a tellerette packed-bed photocatalytic reactor. *Adv Environ Res* **6**:411–418 (2002).
- Dutta PK and Ray AK, Experimental investigation of Taylor vortex photocatalytic reactor for water purification. *Chem Eng Sci* **59**:5249–5259 (2004).
- Szczecowski JG, Koval CA and Noble RD, A Taylor vortex reactor for heterogeneous photocatalysis. *Chem Eng Sci* **50**:3163–3173 (1995).
- Giordano RC, Giordano RLC, Prazeres DMF and Cooney CL, Analysis of a Taylor-Poiseuille vortex flow reactor – I: Flow patterns and mass transfer characteristics. *Chem Eng Sci* **53**:3635–3652 (1998).
- Richter O, Hoffmann H and Kraushaar-Czarnetzki B, Effect of the rotor shape on the mixing characteristics of a continuous flow Taylor-vortex reactor. *Chem Eng Sci* **63**:3504–3513 (2008).
- Kuo HP, Wu CT and Hsu RC, Continuous reduction of toluene vapours from the contaminated gas stream in a fluidised bed photoreactor. *Powder Technol* **195**:50–56 (2009).
- Lee D-K, Kim S-C, Cho I-C, Kim S-J and Kim S-W, Photocatalytic oxidation of microcystin-LR in a fluidized bed reactor having TiO_2 -coated activated carbon. *Sep Purif Technol* **34**:59–66 (2004).
- Peill NJ and Hoffmann MR, Development and optimization of a TiO_2 -coated fiber-optic cable reactor: photocatalytic degradation of 4-chlorophenol. *Environ Sci Technol* **29**:2974–2981 (1995).
- Li Puma G and Yue PL, Comparison of the effectiveness of photon-based oxidation processes in a pilot falling film photoreactor. *Environ Sci Technol* **33**:3210–3216 (1999).
- D. Bockelmann RG, Weichgrebe D and Bahnemann D, Solar detoxification of polluted water: comparing the efficiencies of a parabolic through reactor and a novel thin-film fixed-bed reactor, in *Photocatalytic Purification and Treatment of Water and Air*, ed by Ollis DF and Al-Ekabi H. Elsevier Science, Amsterdam, The Netherlands, 771–776 (1993).
- Sahle-Demessie E, Bekele S and Pillai UR, Residence time distribution of fluids in stirred annular photoreactor. *Catal Today* **88**:61–72 (2003).
- Zhang Z, Anderson WA and Moo-Young M, Experimental analysis of a corrugated plate photocatalytic reactor. *Chem Eng J* **99**:145–152 (2004).
- Dijkstra MFJ, Michorius A, Buwalda H, Panneman HJ, Winkelman JGM and Beenackers AACM, Comparison of the efficiency of immobilized and suspended systems in photocatalytic degradation. *Catal Today* **66**:487–494 (2001).
- Chong MN, Jin B, Zhu HY, Chow CWK and Saint C, Application of H-titanate nanofibers for degradation of Congo Red in an annular slurry photoreactor. *Chem Eng J* **150**:49–54 (2009).
- Augugliaro V, Loddo V, Palmisano L and Schiavello M, Performance of heterogeneous photocatalytic systems: influence of operational

- variables on photoactivity of aqueous suspension of TiO_2 . *J Catal* **153**:32–40 (1995).
- 42 Minero C and Vione D, A quantitative evaluation of the photocatalytic performance of TiO_2 slurries. *Appl Catal B: Environ* **67**:257–269 (2006).
 - 43 Ollis DF, Pelizzetti E and Serpone N, Photocatalyzed destruction of water contaminants. *Environ Sci Technol* **25**:1522–1529 (1991).
 - 44 Ray AK and Beenackers AACM, Novel swirl-flow reactor for kinetic studies of semiconductor photocatalysis. *AIChE J* **43**:2571–2578 (1997).
 - 45 Chen D, Li F and Ray AK, External and internal mass transfer effect on photocatalytic degradation. *Catal Today* **66**:475–485 (2001).
 - 46 Pruden AL and Ollis DF, Degradation of chloroform by photoassisted heterogeneous catalysis in dilute aqueous suspensions of titanium dioxide. *Environ Sci Technol* **17**:628–631 (1983).
 - 47 Kormann C, Bahnemann DW and Hoffmann MR, Photolysis of chloroform and other organic molecules in aqueous titanium dioxide suspensions. *Environ Sci Technol* **25**:494–500 (1991).
 - 48 Pramauro E, Vincenti M, Augugliaro V and Palmisano L, Photocatalytic degradation of Monuron in aqueous titanium dioxide dispersions. *Environ Sci Technol* **27**:1790–1795 (1993).
 - 49 Pathirana HMKK and Maithreepala RA, Photodegradation of 3,4-dichloropropionamide in aqueous TiO_2 suspensions. *J Photochem Photobiol A: Chem* **102**:273–277 (1997).
 - 50 Li Puma G and Yue PL, Photocatalytic oxidation of chlorophenols in single-component and multicomponent systems. *Ind Eng Chem Res* **38**:3238–3245 (1999).
 - 51 Li Puma G and Yue PL, Enhanced photocatalysis in a pilot laminar falling film slurry reactor. *Ind Eng Chem Res* **38**:3246–3254 (1999).
 - 52 San N, Hatipoglu A, Koçtürk G and Çınar Z, Prediction of primary intermediates and the photodegradation kinetics of 3-aminophenol in aqueous TiO_2 suspensions. *J Photochem Photobiol A: Chem* **139**:225–232 (2001).
 - 53 Jeon J, Kim S, Lim T and Lee D, Degradation of trichloroethylene by photocatalysis in an internally circulating slurry bubble column reactor. *Chemosphere* **60**:1162–1168 (2005).
 - 54 Sauer T, Cesconeto Neto G, José HJ and Moreira RFP, Kinetics of photocatalytic degradation of reactive dyes in a TiO_2 slurry reactor. *J Photochem Photobiol A: Chem* **149**:147–154 (2002).
 - 55 Kamble SP, Sawant SB and Pangarkar VG, Photocatalytic mineralization of phenoxyacetic acid using concentrated solar radiation and titanium dioxide in slurry photoreactor. *Chem Eng Res Design* **84**:355–362 (2006).
 - 56 Adams M, Campbell I and Robertson PKJ, Novel Photocatalytic reactor development for removal of hydrocarbons from water. *Int J Photoenergy* Volume 2008 7 pages (2008).
 - 57 Robertson PKJ, Campbell I and Russell D, Photocatalytic Reactor – Apparatus and Method for Treating Fluid by Means of a Treatment Container. International Patent Publication Number WO 2005/033016, publication date 29 September 2004.
 - 58 McCullagh C, Robertson PKJ, Adams M, Pollard PM and Mohammed A, Development of a slurry continuous flow reactor for photocatalytic treatment of industrial waste water. *J Photochem Photobiol A: Chem* **211**:42–46 (2010).
 - 59 Salu OA, Adams M, Robertson PKJ, Wong LS and McCullagh C, Remediation of oily wastewater from an interceptor tank using a novel photocatalytic drum reactor. *Desal Water Treatment* **26**:1–5 (2011).
 - 60 Chen D and Ray AK, Photocatalytic kinetics of phenol and its derivatives over UV irradiated TiO_2 . *Appl Catal B: Environ* **23**:143–157 (1999).
 - 61 Martin ST, Herrmann H, Choi WY and Hoffmann MR, Time-resolved microwave conductivity. Part 1. TiO_2 photoreactivity and size quantization. *J Chem Soc Faraday Trans* **90**:3315–3322 (1994).
 - 62 Mehrotra K, Yablonsky GS and Ray AK, Kinetic studies of photocatalytic degradation in a TiO_2 slurry system: distinguishing working regimes and determining rate dependences. *Ind Eng Chem Res* **42**:2273–2281 (2003).
 - 63 Moreira R, Sauer T, Casaril L and Humeres E, Mass transfer and photocatalytic degradation of leather dye using TiO_2 /UV. *J Appl Electrochem* **35**:821–829 (2005).
 - 64 Ballari MdIM, Alfano OM and Cassano AE, Mass transfer limitations in slurry photocatalytic reactors: experimental validation. *Chem Eng Sci* **65**:4931–4942 (2010).
 - 65 Paz Y, Application of TiO_2 photocatalysis for air treatment: patents' overview. *Appl Catal B: Environ* **99**:448–460 (2010).
 - 66 Dibble LA and Raupp GB, Fluidized-bed photocatalytic oxidation of trichloroethylene in contaminated air streams. *Environ Sci Technol* **26**:492–495 (1992).
 - 67 Lim TH and Kim SD, Trichloroethylene degradation by photocatalysis in annular flow and annulus fluidized bed photoreactors. *Chemosphere* **54**:305–312 (2004).
 - 68 Lim TH and Kim SD, Photocatalytic degradation of trichloroethylene (TCE) over TiO_2 /silica gel in a circulating fluidized bed (CFB) photoreactor. *Chem Eng Process* **44**:327–334 (2005).
 - 69 Rodríguez Couto S, Domínguez A and Sanromán A, Photocatalytic degradation of dyes in aqueous solution operating in a fluidized bed reactor. *Chemosphere* **46**:83–86 (2002).
 - 70 Son Y-H, Jeon M-K, Ban J-Y, Kang M and Choung S-J, Application of three-phase fluidized photocatalytic system to decompositions of acetic acid and ammonia. *J Ind Eng Chem* **11**:938–944 (2005).
 - 71 Kang M, Synthesis of Fe/TiO_2 photocatalyst with nanometer size by solvothermal method and the effect of H_2O addition on structural stability and photodecomposition of methanol. *J Mol Catal A: Chem* **197**:173–183 (2003).
 - 72 Nelson RJ, Flakker CL and Muggli DS, Photocatalytic oxidation of methanol using titania-based fluidized beds. *Appl Catal B: Environ* **69**:189–195 (2007).
 - 73 Gao H-T, Si C-D and Liu G-J, Sound assisted photocatalytic degradation of formaldehyde in fluidized bed reactor. *J Taiwan Inst Chem Eng* **42**:108–113 (2011).
 - 74 Vorontsov AV, Savinov E and Smirniotis PG, Vibrofluidized- and fixed-bed photocatalytic reactors: case of gaseous acetone photooxidation. *Chem Eng Sci* **55**:5089–5098 (2000).
 - 75 Lim TH, Jeong SM, Kim SD and Gyeon J, Photocatalytic decomposition of NO by TiO_2 particles. *J Photochem Photobiol A: Chem* **134**:209–217 (2000).
 - 76 Foster NR and Bassiti K, Photocatalytic Reactor. European Patent – EP2089328 (A1), World Patent – WO2008050119(1998) (2008).
 - 77 Al-Ekabi H and Serpone N, Kinetics studies in heterogeneous photocatalysis. I. Photocatalytic degradation of chlorinated phenols in aerated aqueous solutions over titania supported on a glass matrix. *J Phys Chem* **92**:5726–5731 (1988).
 - 78 Nogueira RFP and Jardim WF, TiO_2 -fixed-bed reactor for water decontamination using solar light. *Solar Energy* **56**:471–477 (1996).
 - 79 Ray AK and Beenackers AACM, Development of a new photocatalytic reactor for water purification. *Catal Today* **40**:73–83 (1998).
 - 80 Feitz AJ, Boyden BH and Waite TD, Evaluation of two solar pilot scale fixed-bed photocatalytic reactors. *Water Res* **34**:3927–3932 (2000).
 - 81 Dionysiou DD, Balasubramanian G, Suidan MT, Khodadoust AP, Baudin I and Lainé J-M, Rotating disk photocatalytic reactor: development, characterization, and evaluation for the destruction of organic pollutants in water. *Water Res* **34**:2927–2940 (2000).
 - 82 Dionysiou DD, Khodadoust AP, Kern AM, Suidan MT, Baudin I and Lainé J-M, Continuous-mode photocatalytic degradation of chlorinated phenols and pesticides in water using a bench-scale TiO_2 rotating disk reactor. *Appl Catal B: Environ* **24**:139–155 (2000).
 - 83 Hamill NA, Weatherley LR and Hardacre C, Use of a batch rotating photocatalytic contactor for the degradation of organic pollutants in wastewater. *Appl Catal B: Environ* **30**:49–60 (2001).
 - 84 Dionysiou DD, Suidan MT, Baudin I and Lainé J-M, Oxidation of organic contaminants in a rotating disk photocatalytic reactor: reaction kinetics in the liquid phase and the role of mass transfer based on the dimensionless Damköhler number. *Appl Catal B: Environ* **38**:1–16 (2002).
 - 85 Villacres R, Ikeda S, Torimoto T and Ohtani B, Development of a novel photocatalytic reaction system for oxidative decomposition of volatile organic compounds in water with enhanced aeration. *J Photochem Photobiol A: Chem* **160**:121–126 (2003).
 - 86 Zhang L, Kanki T, Sano N and Toyoda A, Development of TiO_2 photocatalyst reaction for water purification. *Sep Purif Technol* **31**:105–110 (2003).
 - 87 McMurray TA, Byrne JA, Dunlop PSM, Winkelman JGM, Eggins BR and McAdams ET, Intrinsic kinetics of photocatalytic oxidation of formic and oxalic acid on immobilised TiO_2 films. *Appl Catal A: Gen* **262**:105–110 (2004).
 - 88 Lin HF and Valsaraj KT, A titania thin film annular photocatalytic reactor for the degradation of polycyclic aromatic hydrocarbons in dilute water streams. *J Hazard Mater* **99**:203–219 (2003).

- 89 Mozia S, Tomaszewska M and Morawski AW, Photocatalytic degradation of azo-dye Acid Red 18. *Desalination* **185**:449–456 (2005).
- 90 Mozia S, Tomaszewska M and Morawski AW, Photodegradation of azo dye Acid Red 18 in a quartz labyrinth flow reactor with immobilized TiO₂ bed. *Dyes Pigments* **75**:60–66 (2007).
- 91 Du P, Carneiro JT, Moulijn JA and Mul G, A novel photocatalytic monolith reactor for multiphase heterogeneous photocatalysis. *Appl Catal A: Gen* **334**:119–128 (2008).
- 92 Carneiro JT, Berger R, Moulijn JA and Mul G, An internally illuminated monolith reactor: pros and cons relative to a slurry reactor. *Catal Today* **147**:S324–S329 (2009).
- 93 Nguyen T-V and Wu JCS, Photoreduction of CO₂ to fuels under sunlight using optical-fiber reactor. *Solar Energy Mater Solar Cells* **92**:864–872 (2008).
- 94 Hajiesmaili S, Josset S, Bégin D, Pham-Huu C, Keller N and Keller V, 3D solid carbon foam-based photocatalytic materials for vapor phase flow-through structured photoreactors. *Appl Catal A: Gen* **382**:122–130 (2010).
- 95 Salas M, Serrano B and de Lasa HI, Experimental evaluation of photon absorption in an aqueous TiO₂ slurry reactor. *Chem Eng J* **90**:219–229 (2002).
- 96 Ochuma JJ, Osibo OO, Fishwick RP, Pollington S, Wagland A and Wood J, *et al*, Three-phase photocatalysis using suspended titania and titania supported on a reticulated foam monolith for water purification. *Catal Today* **128**:100–107 (2007).
- 97 van Grieken R, Marugán J, Sordo C and Pablos C, Comparison of the photocatalytic disinfection of *E. coli* suspensions in slurry, wall and fixed-bed reactors. *Catal Today* **144**:48–54 (2009).
- 98 Dillert R, Cassano AE, Goslich R and Bahnemann D, Large scale studies in solar catalytic wastewater treatment. *Catal Today* **54**:267–282 (1999).
- 99 Benz V, Müller M, Bahnemann DW, Weichgrebe D and Brehm M, Reaktoren für die photokatalytische Abwasserreinigung mit Stegmehrfachplatten als Solarelemente. *Deutsche Offenlegungsschrift* DE 195 14 372 A1 (1996).
- 100 Dillert R, Vollmer S, Gross E, Schöber M, Bahnemann D and Wienefeld J, *et al*, Solar-catalytic treatment of an industrial wastewater. *Zeitschrift für Physikalische Chemie* **213**:141–147 (1999).
- 101 Imoberdorf GE, Cassano AE, Irazoqui HA and Alfano OM, Optimal design and modeling of annular photocatalytic wall reactors. *Catal Today* **129**:118–126 (2007).
- 102 Shu H-Y and Chang M-C, Pilot scale annular plug flow photoreactor by UV/H₂O₂ for the decolorization of azo dye wastewater. *J Hazard Mater* **125**:244–251 (2005).
- 103 van Well M, Dillert RHG, Bahnemann DW, Benz VW and Mueller MA, A novel nonconcentrating reactor for solar water detoxification. *J Solar Energy Eng* **119**:114–119 (1997).
- 104 Mozia S, Morawski AW, Toyoda M and Inagaki M, Effectiveness of photodecomposition of an azo dye on a novel anatase-phase TiO₂ and two commercial photocatalysts in a photocatalytic membrane reactor (PMR). *Sep Purif Technol* **63**:386–391 (2008).
- 105 Alexiadis A and Mazzarino I, Design guidelines for fixed-bed photocatalytic reactors. *Chem Eng Process* **44**:453–459 (2005).
- 106 Cernigoi U, Stangar UL and Trebse P, Evaluation of a novel Carberry type photoreactor for the degradation of organic pollutants in water. *J Photochem Photobiol A: Chem* **188**:169–176 (2007).
- 107 Lo C-C, Hung C-H, Yuan C-S and Wu J-F, Photoreduction of carbon dioxide with H₂ and H₂O over TiO₂ and ZrO₂ in a circulated photocatalytic reactor. *Solar Energy Mater Solar Cells* **91**:1765–1774 (2007).
- 108 Fu J, Ji M, Zhao Y and Wang L, Kinetics of aqueous photocatalytic oxidation of fulvic acids in a photocatalysis-ultrafiltration reactor (PUR). *Separ Purif Technol* **50**:107–113 (2006).
- 109 Li Puma G and Lock Yue P, The modeling of a fountain photocatalytic reactor with a parabolic profile. *Chem Eng Sci* **56**:721–726 (2001).
- 110 Agarwal A and Bhaskarwar AN, Comparative simulation of falling-film and parallel-film reactors for photocatalytic production of hydrogen. *Int J Hydro Energy* **32**:2764–2775 (2007).
- 111 Ochuma JJ, Fishwick RP, Wood J and Winterbottom JM, Photocatalytic oxidation of 2,4,6-trichlorophenol in water using a cocurrent downflow contactor reactor (CDCR). *J Hazard Mater* **144**:627–633 (2007).
- 112 Chin SS, Lim TM, Chiang K and Fane AG, Hybrid low-pressure submerged membrane photoreactor for the removal of bisphenol A. *Desalination* **202**:253–261 (2007).
- 113 Orozco SL, Arancibia-Bulnes CA and Suárez-Parra R, Radiation absorption and degradation of an azo dye in a hybrid photocatalytic reactor. *Chem Eng Sci* **64**:2173–2185 (2009).
- 114 Erdei L, Arcachakul N and Vigneswaran S, A combined photocatalytic slurry reactor-immersed membrane module system for advanced wastewater treatment. *Separ Purif Technol* **62**:382–388 (2008).
- 115 Hao X-G, Li H-H, Zhang Z-L, Fan C-M, Liu S-B and Sun Y-P, Modeling and experimentation of a novel labyrinth bubble photoreactor for degradation of organic pollutant. *Chem Eng Res Des* **87**:1604–1611 (2009).
- 116 Pourahmad A, Sohrabnezhad S and Kashefian E, AgBr/nanoAIMCM-41 visible light photocatalyst for degradation of methylene blue dye. *Spectrochim Acta Part A: Mol Biomol Spectrosc* **77**:1108–1114.
- 117 Shifu C, Wei Z, Wei L, Huaye Z, Xiaoling Y and Yinghao C, Preparation, characterization and activity evaluation of p-n junction photocatalyst p-CaFe₂O₄/n-Ag₃VO₄ under visible light irradiation. *J Hazard Mater* **172**:1415–1423 (2009).
- 118 Liu W, Ji M and Chen S, Preparation, characterization and activity evaluation of Ag₂Mo₄O₁₃ photocatalyst. *J Hazard Mater* **186**:2001–2008 (2010).
- 119 Kanade KG, Baeg J-O, Kale BB, Mi Lee S, Moon S-J and Kong K-J, Rose-red color oxynitride Nb₂Zr₆O₁₇-xN_x: a visible light photocatalyst to hydrogen production. *Int J Hydrogen Energy* **32**:4678–4684 (2007).
- 120 Jing D, Liu M, Chen Q and Guo L, Efficient photocatalytic hydrogen production under visible light over a novel W-based ternary chalcogenide photocatalyst prepared by a hydrothermal process. *Int J Hydrogen Energy* **35**(1):8521–8527 (2010).
- 121 Shen S, Zhao L and Guo L, Cetyltrimethylammoniumbromide (CTAB)-assisted hydrothermal synthesis of ZnIn₂S₄ as an efficient visible-light-driven photocatalyst for hydrogen production. *Int J Hydrogen Energy* **33**:4501–4510 (2008).